Volume 14
Number 40
28 October 2022
Pages 14813-15204

Nanoscale

rsc.li/nanoscale

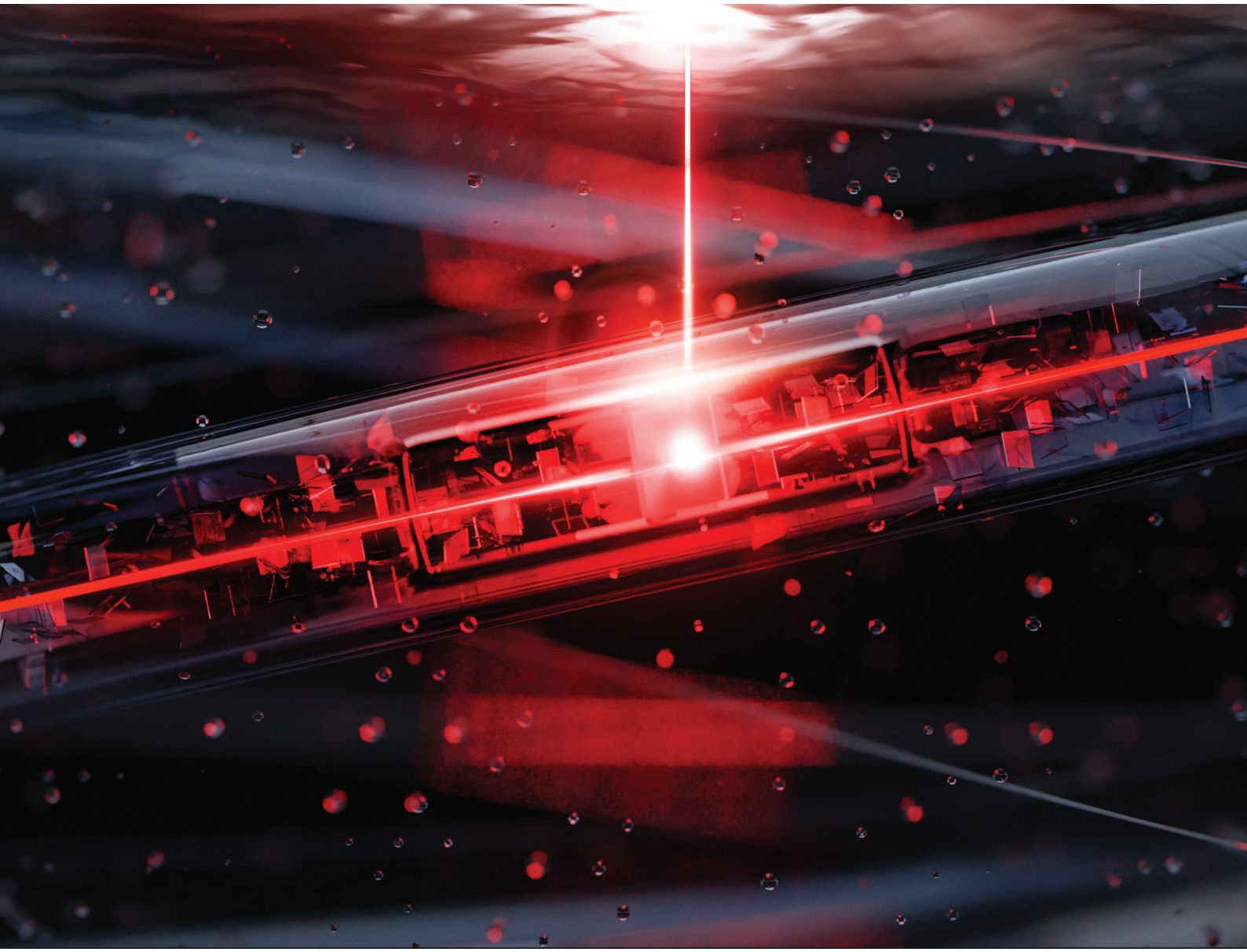

ISSN 2040-3372

ROYAL SOCIETY OF CHEMISTRY

COMMUNICATION
Hilmi Volkan Demir *et al.*
Observation of optical gain from aqueous quantum well heterostructures in water

NCNST

Nanoscale

COMMUNICATION

View Article Online
View Journal | View Issue

Cite this: *Nanoscale*, 2022, **14**, 14895

Received 4th July 2022,
Accepted 2nd September 2022

DOI: 10.1039/d2nr03659b

rsc.li/nanoscale

Observation of optical gain from aqueous quantum well heterostructures in water†

Savas Delikanli,‡[a,b] Furkan Isik, ‡[b] Emek G. Durmusoglu,[a] Onur Erdem,[b] Farzan Shabani,[b] Betul Canimkurbey, [b,c] Satish Kumar,[b] Hamed Dehghanpour Baruj[b] and Hilmi Volkan Demir *[a,b]

Although achieving optical gain using aqueous solutions of colloidal nanocrystals as a gain medium is exceptionally beneficial for bio-optoelectronic applications, the realization of optical gain in an aqueous medium using solution-processed nanocrystals has been extremely challenging because of the need for surface modification to make nanocrystals water dispersible while still maintaining their gain. Here, we present the achievement of optical gain in an aqueous medium using an advanced architecture of CdSe/CdS@$Cd_xZn_{1-x}S$ core/crown@gradient-alloyed shell colloidal quantum wells (CQWs) with an ultralow threshold of ~3.4 μJ cm^{-2} and an ultralong gain lifetime of ~2.6 ns. This demonstration of optical gain in an aqueous medium is a result of the carefully heterostructured CQWs having large absorption cross-section and gain cross-section in addition to inherently slow Auger recombination in these CQWs. Furthermore, we show low-threshold in-water amplified spontaneous emission (ASE) from these aqueous CQWs with a threshold of 120 μJ cm^{-2}. In addition, we demonstrate a whispering gallery mode laser with a low threshold of ~30 μJ cm^{-2} obtained by incorporating films of CQWs by exploiting layer-by-layer approach on a fiber. The observation of low-threshold optical gain with ultralong gain lifetime presents a significant step toward the realization of advanced optofluidic colloidal lasers and their continuous-wave pumping.

Introduction

Colloidal semiconductor nanocrystals (NCs) are highly promising as optical gain media thanks to their size-dependent spectral tunability, solution processability and compatibility to various matrices.[1,2] After the first demonstration of amplified spontaneous emission (ASE) from their close-packed solid films two decades ago,[3] semiconductor NCs in various geometries and compositions have been utilized and investigated as gain media.[4–6] Although in-solution optical gain can be highly advantageous owing to its potential practical applications, including sensing and detection,[7–9] there are only a few reports and demonstrations of in-solution optical gain and a limited number of in-solution lasing compared to optical gain and lasing studies using close-packed films of NCs.[10–15] This is primarily due to the low concentration of gain media possible in solution which is constraining the realization of ASE. The need for high concentration is principally a consequence of the difficulty of achieving ASE build-up time, which strongly depends both on the gain cross-section and the concentration of the gain material in-solution,[3] faster than the Auger lifetime which is unfortunately very efficient in nanocrystals unlike bulk structures.[3,4] Nevertheless, solution-based gain using colloidal nanocrystals is very valuable because of its greater photostability thanks to the continuous renewal of the gain medium because of the constant movement of nanocrystals and ease of incorporation into various optical cavities. Such solution-based gain medium can be easily incorporated into optofluidic lasers for sensitive detection of chemicals and biological materials and on-chip imaging.

Recently, colloidal quantum wells (CQWs) have emerged as a favorable optical gain medium since they possess large absorption cross-sections,[16–18] with continuously tunable emission,[19,20] suppressed Auger recombination rates,[17,21] low optical gain thresholds,[17,22,23] long gain lifetimes,[17] and large gain cross-sections.[14,15] Especially, their large gain cross-section makes them excellent candidates for in-solution lasing by supporting the gain condition and feasible levels of gain

[a]*Luminous! Center of Excellence for Semiconductor Lighting and Displays, School of Electrical and Electronic Engineering, School of Physical and Mathematical Sciences, School of Materials Science and Engineering, Nanyang Technological University, 50 Nanyang Avenue, Singapore 639798, Singapore. E-mail: hvdemir@ntu.edu.sg, volkan@bilkent.edu.tr*

[b]*Department of Electrical and Electronics Engineering, Department of Physics, UNAM – Institute of Materials Science and Nanotechnology, Bilkent University, Ankara 06800, Turkey*

[c]*Serefeddin Health Services Vocational School, Central Research Laboratory, Amasya University, Amasya 05100, Turkey*

†Electronic supplementary information (ESI) available. See DOI: https://doi.org/10.1039/d2nr03659b

‡These authors contributed equally to this work.

coefficients in solution.[14] Recently, ASE in solution and lasing in microfluidic channels have been demonstrated using CQWs dispersed in non-polar solvents with record low thresholds, almost one order of magnitude better than the previous lasing demonstrations from colloidal nanocrystals.[11,14,15] This low threshold optical gain from these CQWs is significantly important for realization of stable high-quality lasers in microfluidic devices for numerous applications, including biological and chemical sensors, flow cytometry and the development of advanced lab-on-chip (LOC) devices. In addition, recently introduced water-based semiconductor CQWs, which can be obtained by synthesizing them in organic solvents and then transferring them to water *via* ligand exchange, present an attractive platform for optical gain applications thanks to their photostability, highly efficient emission and soft confinement potential owing to their gradient alloyed shell.[24] Although these exciting aqueous CQWs present an extraordinary platform for in-solution optical gain, their optical gain properties have never been explored to date.

In this study, we demonstrate the achievement of optical gain in an aqueous medium using an advanced heterostructure of CdSe/CdS@$Cd_xZn_{1-x}S$ core/crown@gradient-alloyed shell colloidal CQWs employing ultrafast transient absorption technique with a threshold of 3.4 μJ cm^{-2}. These nanocrystals exhibit a long gain lifetime of 2.6 ns which makes them superior candidates for achieving optical gain under CW and quasi-CW pumping. This extremely long gain lifetime can be attributed to the smooth confinement potential suppressing the Auger recombination. We also demonstrated in-solution ASE from these carefully heterostructured aqueous colloidal nanocrystals using a capillary tube with a threshold of ~120 μJ cm^{-2}. In addition, we show whispering gallery mode (WGM) laser with a threshold of ~30 μJ cm^{-2} obtained by incorporating films of our CQWs on a fiber using layer-by-layer approach by taking advantage of their 2D geometry, short mercaptopropionic acid (MPA) ligands allowing higher packing density of CQWs and carboxylic end groups of their ligands causing hydrophilicity. The layer-by-layer approach leads to a uniform film on the lateral surface of the fiber and hence a much lower lasing threshold in this work compared to the previous report[25] in which films were obtained by assistance of capillary force. In this WGM laser, the lasing is strongly guided along the fiber and hence exhibits a spatially coherent emission. This solution-processed architecture of aqueous CQWs with their extraordinary properties makes excellent gain media for the design of CW-pumped lasers and the achievement of much needed optical gain in water is a major step forward for development of advanced optofluidic lasers in biocompatible environments.

Results and discussion

In this work, we synthesized CdSe/CdS@$Cd_{1-x}Zn_xS$ core/crown@gradient-alloyed shell (C/C@GS) CQWs by growing 4 monolayers of $Cd_{1-x}Zn_xS$ shells on 4 monolayer thick CdSe/CdS core/crown CQWs using colloidal atomic layer deposition (c-ALD) technique.[24,26] Then, we made them water dispersible by passivating their surface with MPA *via* ligand exchange as described in our previous work.[24] Details of the syntheses and ligand exchange procedures are presented in ESI.† The quantum yield of these aqueous C/C@GS CQWs is approximately 90%. In this architecture, $Cd_{1-x}Zn_xS$ gradient-alloyed shells grown on the seed CdSe/CdS core/crown CQWs provide a soft confinement potential and hole wavefunction is largely localized in the core region due to the large band-offset while electron is largely relaxed into the $Cd_{1-x}Zn_xS$ shells layers as a result of small conduction band-offset and smaller effective mass.[17,24] This spatial difference between the electron and hole wavefunctions generates a quasi-type-II band alignment. The schematic of C/C@GS CQWs together with the band-offsets of the heterostructure is presented in Fig. 1a. A representative transmission electron microscopy (TEM) image of C/C@GS CQWs is provided in Fig. 1b and energy dispersive spectroscopy (EDS) maps of cadmium, selenium, sulfur, and zinc from a single CQW (shown in the inset) are presented in Fig. 1c. As can be seen in here, selenium is located only at the core but sulfur, zinc and cadmium are present all over the CQW as expected from alloyed shell of CdZnS in these CQWs.[24] The absorption and photoluminescence (PL) spectra of aqueous CQWs are shown in Fig. 1d. The peaks appearing at 625 and 575 nm in the absorption spectrum are associated with the heavy-hole and light-hole excitonic transitions, respectively. The PL emission peak of these aqueous CQWs is located at 629.6 nm and the full-width-half-maximum (FWHM) of the PL is 19.6 nm.

Fig. 2a presents non-linear absorption spectra $\alpha = \Delta\alpha + \alpha_0$, where $\Delta\alpha$ is the absorption bleach and α_0 is the absorption of the unexcited sample, parametrized with respect to the average number of generated excitons per CQW (given in the legend). In here, we used the absorption bleach spectra at ~15 ps. The average number of photogenerated excitons per CQW $\langle N_0 \rangle$ is calculated by using $N_0 = f \times \sigma$, where f is the pump fluence and σ is the absorption cross-section. Absorption cross-section of our sample is 2.0×10^{-13} cm^2 and was calculated by following a method explained in our previous work.[16] The non-linear absorption spectra gradually decrease as we increase the pump fluence as can be seen in Fig. 2a and α becomes negative at the wavelengths within the proximity of the stimulated emission. This negative net absorption, $\alpha < 0$, signifies the occurrence of optical gain.[3] The optical gain occurs initially at 640 nm and then as the pump fluence is further increased, the peak of the net negative absorption slowly blue-shifts to 630 nm. This blue shift is a signature of stimulated emission from higher order excitons.[27,28] In Fig. 2b, the absorption α of our aqueous CQWs at the ASE peak as a function of the average number of photogenerated excitons per CQW $\langle N_0 \rangle$ is provided. The change in the sign of α indicates the threshold for achieving stimulated emission and thus our threshold for stimulated emission is $\langle N_0 \rangle \approx 1.4$ excitons which corresponds to pump fluence of 3.4 μJ cm^{-2}.

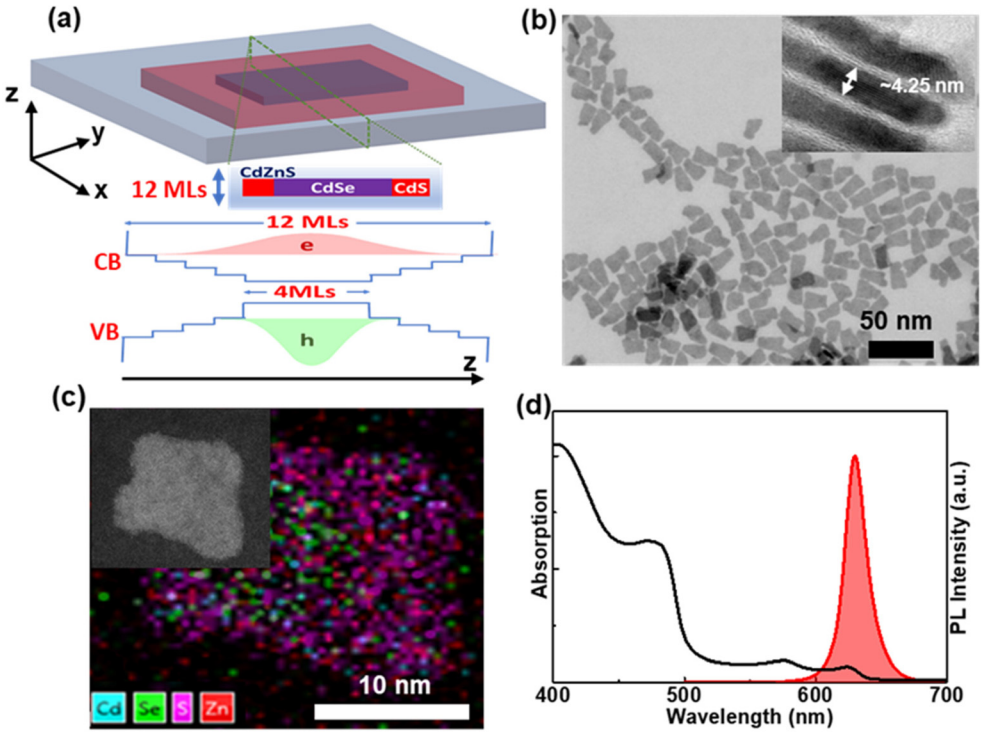

Fig. 1 (a) A schematic of CdSe/CdS@$Cd_xZn_{1-x}S$ core/crown@gradient-alloyed shell colloidal quantum wells (CQWs) together with the band-offsets. (b) A representative transmission electron microscopy (TEM) image of C/C@GS CQWs. (c) EDS maps of cadmium, selenium, sulfur, and zinc from a single CQW (shown in the inset). (d) Absorption and photoluminescence spectra of the CQWs.

We also investigated the material gain and gain cross-section of these gradient alloyed CQWs. Material gain $g(\mathrm{pf}, \lambda, t)$ at a specific pump fluence is given by

$$g(\mathrm{pf}, \lambda, t) = \alpha(\mathrm{pf}, \lambda, t) \times \mu(\text{at } 400 \text{ nm})/\alpha_0(\text{at } 400 \text{ nm}), \quad (1)$$

where pf is the pump fluence, λ is the wavelength, t is the time, and μ (at 400 nm) is the intrinsic absorption coefficient at 400 nm.[29] Intrinsic absorption coefficient was calculated by dividing the absorption cross-section of our CQWs by its volume and the resulting μ (at 400 nm) is 1.35×10^5 cm^{-1} for our CQWs. The material gain $g(\mathrm{pf}, \lambda, t)$ reaches 6000 cm^{-1} at the pump fluence of 15 μJ cm^{-2}, which corresponds to $\langle N_0 \rangle$ = 6. In addition, we obtained the gain cross-section of these aqueous CQWs. The gain cross-section per CQW (γ_g) can be calculated by

$$g_{\mathrm{net}} = \gamma_g \times C - \alpha, \quad (2)$$

where C is the concentration of CQWs and α is the optical loss coefficient.[14] For the case that we obtained g_{net} (pf = 15 μJ cm^{-2}) = 6000 cm^{-1}, C is $\sim 5 \times 10^{17}$ cm^{-3}. Here, we can easily assume that the net modal gain is close to the modal gain (g) since loss coefficient from the films of CQWs is very small (in the order of 10 cm^{-1})[30] compared to the net modal gain. Then, γ_g (pf = 15 μJ cm^{-2}) was calculated to be 1.2×10^{-14} cm^2. This is smaller than the reported value from CdSe/CdS core/shell CQWs, which is likely obtained at higher fluences,[14] but 1 to 2 orders of magnitude larger than those of QDs and nanorods.[3,10]

In Fig. 2c, the 2D time–wavelength colored map of non-linear absorption spectrum of our CQWs is provided at pump fluence of 15 μJ cm^{-2}, corresponding to $\langle N_0 \rangle \approx 6$ for only the region under the optical gain. In this figure, while the coordinates that exhibit optical gain is colored and shown, the coordinates which are not under optical gain is kept white. The spectral position where the maximum gain occurs red-shifts as the time passes as can be seen from Fig. 2c. Initially α is minimum (maximum in magnitude) at 630 nm, slowly shifting towards ~640 nm (at ~2 ns). This spectral red shift of α over time is due to the reduction in the number of excitons with time in the CQWs after their initial generation with the femtosecond pulse. Likely, this is because of the coulombic repulsive forces due to presence of multi-excitons. Then, as the number of excitons decreases with time, α eventually red-shifts spectrally. As can be seen in Fig. 2c, α still stays negative during our measurement window of 1.95 ns which means our gain lifetime is longer than 1.95 ns. In Fig. 2d, we present $-\Delta\alpha$(at 640 nm)/α_0 as a function of the time at the pump fluence of 15 μJ cm^{-2}. Since our sample was still under the gain within our window of measurement, we extrapolated the experimental data after 1.95 ns by fitting three-exponential decay function. The fit is also included in Fig. 2d. Using our fit, we obtained a gain lifetime of 2.6 ns from our aqueous CQWs. This optical gain lifetime is longer than the previously reported gain life-

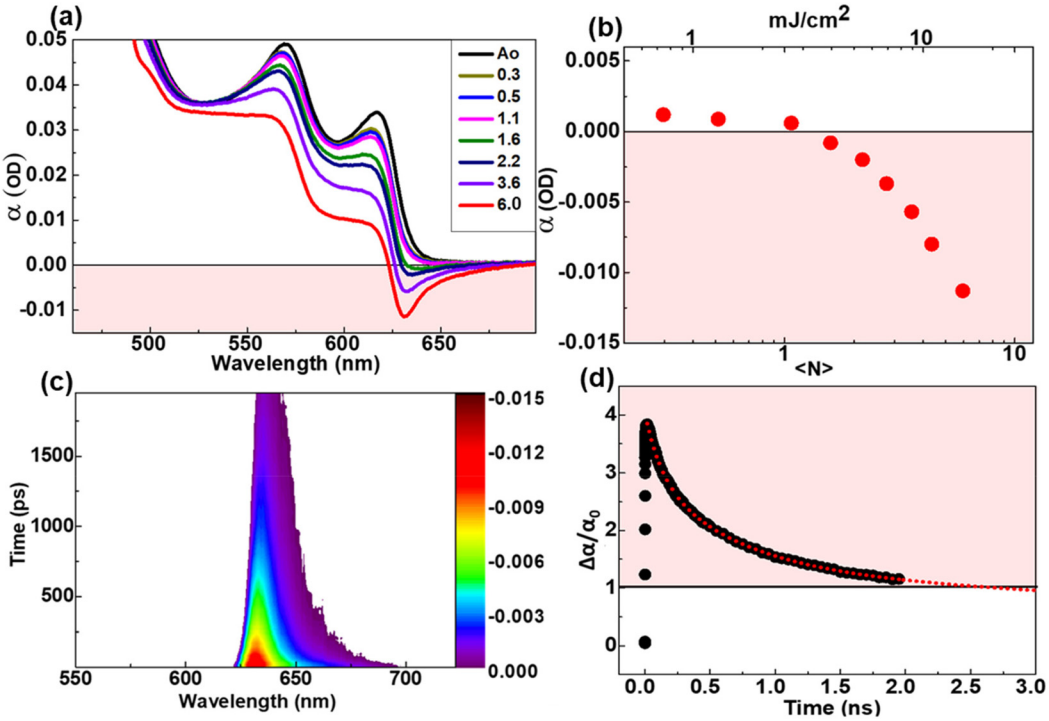

Fig. 2 (a) Nonlinear absorption spectra $\alpha = \Delta\alpha + \alpha_0$, where $\Delta\alpha$ is the absorption bleach and α_0 is the absorption of the unexcited sample, as a function of the average number of generated excitons per CQW. Red-shaded region shows where optical gain occurs ($\alpha < 0$) in this figure. (b) Nonlinear absorption α taken at t = 15 ps as a function of the fluence and average number of generated excitons per CQW. (c) 2D time–wavelength colored map of nonlinear absorption spectrum of our CQWs at pump fluence of 15 μJ cm^{-2}, corresponding to $\langle N_0 \rangle \approx 6$ for the regions only under the optical gain. In (c) only the region exhibiting optical gain is shown and colored, the coordinates which are not under optical gain are colored as white. (d) $-\Delta\alpha$(at 640 nm)/α_0 as a function of the time at the pump fluence of 15 μJ cm^{-2}. In (d) we extrapolate the experimental data after 1.95 ns, which is our experimental temporal window, by fitting with three-exponential decay function, shown in dotted red curve.

times of colloidal quantum wells[17,31,32] and comparable to the best reported gain lifetimes of charged quantum dots[33] and quantum shells.[34] Such elongated gain lifetime in this system can be attributed to the longer Auger lifetimes as a result of the smooth potential confinement provided by the gradient alloyed shell.[4,35] The Auger lifetimes are strongly suppressed in finely graded confinement potentials owing to the significant reduction in the strength of the intraband transition.[4,35]

To explore the in-solution ASE performance of our CQWs, CQWs dispersed in water were placed into a capillary tube having a core size of 300 μm by the assistance of capillary force and then optically pumped with a femtosecond mode-locked laser (pulse width ≈ 120 fs) at 400 nm and 1 kHz repetition rate using a stripe geometry with the help of a cylindrical lens. Emitted photons were collected by using an optical fiber connected to a spectrometer. Pump-fluence dependent ASE spectra from our aqueous CQWs are presented in Fig. 3a. As presented in Fig. 3a, at low pump fluences only the spontaneous emission with a FWHM of ~25 nm appears in the PL spectrum. However, as the pump fluence further is increased, a sharp ASE peak emerges at ~641 nm with a FWHM of ~10 nm for the pump fluences above the threshold and it becomes dominant as the fluence is further increased as can be seen in Fig. 3(a). The blue shift of the ASE can be attributed to the quasi-type-II nature of these CdSe/CdS@Cd$_x$Zn$_{1-x}$S core/crown@gradient-alloyed CQWs, which leads to repulsive interactions in the biexcitonic regime. It is worth mentioning that the degree of such quasi-type-II behavior can be well controlled and fine-tuned by the use of alloying and geometrical parameters, as previously demonstrated in CdSe/Cd$_{1-x}$Zn$_x$S core/shell QDs, nanorods and CQWs.[17,36,37] The emission intensity at the peak as a function of the pump fluence for the CQWs is presented in Fig. 3(b). The ASE threshold obtained in Fig. 3(b) from the super-linear increase of the emission intensity and Fig. 3(a) from the emergence of narrow ASE emission is ~120 μJ cm^{-2}, which is slightly higher than the previously reported ASE threshold of CQWs dispersed in toluene.[15] This is likely due to the difference in the concentration of CQWs and possibly better optical confinement factor of the CQW solution in toluene which has a higher refractive index than water. This lower refractive index of water and low optical quality of the aqueous nanocrystals synthesized before are likely the reasons for the failure in achieving optical gain in water to date. Compared to the nanocrystals dispersed in non-polar solvents, such as hexane and toluene, the optical performance of the nanocrystals dispersed in water falls far behind.[38,39]

To study the stability of the light amplification in our aqueous CQWs, we pumped the sample above the ASE threshold for 4 h continuously. The stability test was per-

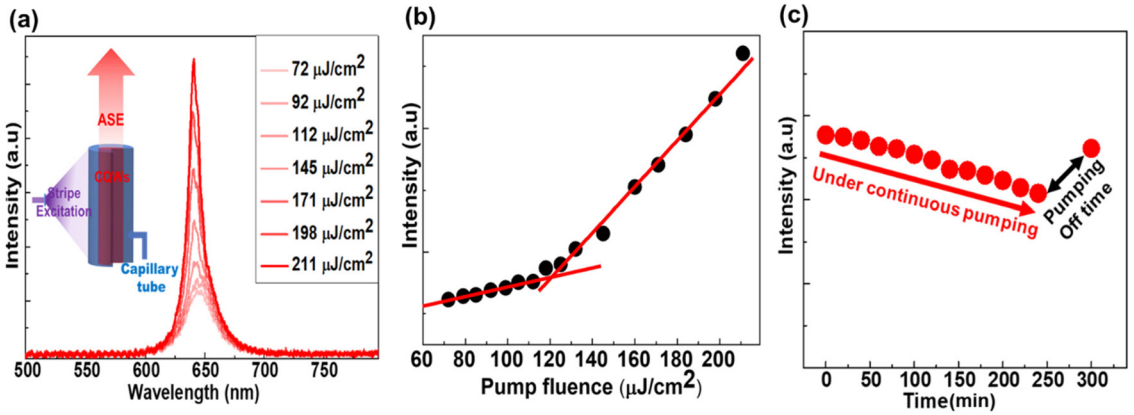

Fig. 3 (a) Pump-fluence dependent in-solution ASE spectra from aqueous CQWs in a capillary tube. Inset of (a) exhibits a schematic of CQW solution in the capillary tube optically excited using stripe geometry for ASE measurements. (b) Emission intensity at the peak as a function of the pump fluence for aqueous CQWs. The crossing point of the fitted red lines in (b) indicates the ASE threshold. (c) ASE intensity as a function of time.

formed under ambient conditions at a threshold of 190 μJ cm^{-2} using a femtosecond mode-locked laser having a pulse width of 150 fs and a 1 kHz repetition rate. We observed a decrease in the ASE intensity with time as presented in Fig. 3c. However, this decrease in the ASE intensity was almost recovered after stopping the optical pumping of the sample for an hour. This phenomenon can be attributed to the dissipation of the heat which accumulated under continuous pumping. As a result, the decrease in the intensity of the ASE under continuous pumping is reversible and largely due to the change in the temperature of the surrounding environment unlike irreversible damage seen in QD microdrop lasers as a result of high fluences needed for obtaining ASE leading photo-oxidation.[12] Hence, our aqueous C/C@GS CQWs offer an effective architecture to considerably improve the optical gain stability problem of colloidal semiconductor nanocrystals thanks to their low in-solution ASE threshold and crown and shell layers for passivation and protection.

Owing to excellent optical gain performance of our engineered aqueous CQWs, we incorporated these CQWs as a gain medium into WGM laser. We obtained the WGM laser by depositing 6 monolayers of aqueous CQWs by layer-by-layer approach on a piece of coreless fiber having a diameter of approximately 125 μm by taking advantage of their 2D geometry and hydrophilicity owing to carboxylic end groups of their ligands. We achieved the deposition of CQWs on fibers by using positively charged poly(diallyldimethylammoniumchloride) (PDDA) linker molecules between each CQW layer as presented in our previous work.[24] The layer-by-layer approach as shown in our previous work leads to uniform film deposition, which is important for lasing applications and other opto-electronic applications, such as light-emitting diodes. Briefly, the surface of the fiber was made hydrophilic by applying oxygen plasma and after that it was dipped into a PDDA linker solution for the attachment of linker molecules to the surface. Then, the fiber was dipped into aqueous CQW solution to attach the CQWs on top of the linker molecules. The process of attaching PDDA and CQWs was repeated 5 more times to reach the desired film thickness on the fiber. The scanning electron microscopy (SEM) image of our WGM laser is displayed in the inset of Fig. 4a, demonstrating that the CQW film obtained by layer-by-layer approach is smooth.

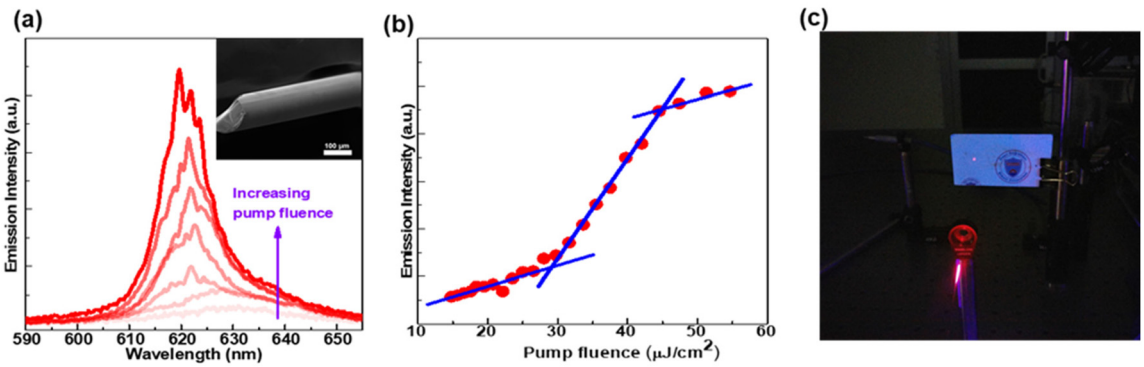

Fig. 4 (a) Luminescence spectra of the CQW integrated fiber. SEM image is given in the inset showing the smoothness of CQW film formation on the lateral sides of the fiber. (b) Pump fluence dependent PL intensity of the CQW integrated fiber. (c) Image of the resulting laser spot from the optically excited CQW integrated fiber.

The emission spectra of the CQW-WGM laser at different pump fluences are given in Fig. 4a. The WGM laser exhibits multimode laser output with each peak approximately having an FWHM of 1.5 nm corresponding to a *Q*-factor of ~413. Emission intensity as a function of the pump fluence is presented in Fig. 4b. The lasing threshold occurs at the pump fluence of ~30 μJ cm^{-2} as can be seen in Fig. 4a and b with the emergence of a sharp peak and superlinear increase of the total intensity. This threshold is lower than the previous result on CQWs based WGM and can be attributed to the higher quality of aqueous CQWs, better film quality on the fiber used in this work obtained by layer-by-layer assembly unlike in the previous work in which the films were obtained by the help of capillary force[25] and short MPA ligands enabling higher packing density of CQWs. This lasing output saturates around ~45 μJ cm^{-2} as can be seen in Fig. 4b. The coherent laser emission of the WGM laser with a well-defined spatial profile is presented in Fig. 4c. In this WGM laser, the lasing emission from WGM resonator is effectively guided along the fiber owing to strong waveguding as also demonstrated in our previous work.[25]

Conclusions

In conclusion, we show the achievement of in-water low-threshold optical gain from our carefully heterostructured aqueous CdSe/CdS@$Cd_xZn_{1-x}S$ core/crown@gradient-alloyed shell CQWs with a threshold of ~3.4 μJ cm^{-2}. These engineered hetero-CQWs exhibit extremely long gain lifetime of around 2.6 ns which makes them particularly advantageous as a gain medium for quasi-CW and CW lasing together with their low-threshold optical gain. This extremely long gain lifetime and ultralow optical gain threshold can be attributed to the smooth confinement potential as a result of their gradient alloyed shell. Using these aqueous CQWs, we also attained in-solution ASE with a threshold of 120 μJ cm^{-2} using capillary tubes. In addition, we demonstrated a low-threshold WGM laser by depositing uniform film of CQWs on a fiber using layer-by-layer approach by exploiting their 2D geometry and hydrophilicity owing to carboxylic end groups of their ligands. In this WGM laser, the lasing is strongly guided along the fiber and hence exhibits a spatially coherent emission. This solution processed aqueous CQWs with their extraordinary electronic properties as a solution-based optical gain medium offers exceptional opportunities for the design of optofluidic lasers for sensitive detection of chemicals and biomedical applications. The achievement of in-water optical gain in this work presents specifically a significant step for biological molecule analyses and detection in the living cells and tissues and other bio-compatible environment.

Author contributions

The manuscript was written through contributions of all authors. S. D. and F. I. contributed equally.

Conflicts of interest

There are no conflicts to declare.

Acknowledgements

The authors gratefully acknowledge the financial support in part from Singapore National Research Foundation under the programs of NRF-NRFI2016-08, the Science and the Singapore Agency for Science, Technology and Research (A*STAR) SERC Pharos Program under grant number 152-73-00025 and Agency for Science, Technology and Research (A*STAR) MTC program under grant number M21J9B0085, Ministry of Education Tier 1 under grant number MOE-RG62/20 (Singapore), and in part from TUBITAK 119N343, 120N076, 121N395 and 20AG001. We also thank Dr Seongwoo Yoo and Dr Zhou Yanyan for providing us with pieces of fiber samples. H. V. D. also acknowledges support from TUBA.

References

1 C. B. Murray, D. J. Norris and M. G. Bawendi, *J. Am. Chem. Soc.*, 1993, **115**, 8706–8715.
2 S. Ithurria, M. D. Tessier, B. Mahler, R. P. S. M. Lobo, B. Dubertret and A. L. Efros, *Nat. Mater.*, 2011, **10**, 936.
3 V. I. Klimov, A. A. Mikhailovsky, S. Xu, A. Malko, J. A. Hollingsworth, C. A. Leatherdale, H.-J. Eisler and M. G. Bawendi, *Science*, 2000, **290**, 314–317.
4 J. M. Pietryga, Y.-S. Park, J. Lim, A. F. Fidler, W. K. Bae, S. Brovelli and V. I. Klimov, *Chem. Rev.*, 2016, **116**, 10513–10622.
5 Y.-S. Park, J. Roh, B. T. Diroll, R. D. Schaller and V. I. Klimov, *Nat. Rev. Mater.*, 2021, **6**, 382–401.
6 M. Sharma, S. Delikanli and H. V. Demir, *Proc. IEEE*, 2020, **108**, 655–675.
7 X. Fan and S.-H. Yun, *Nat. Methods*, 2014, **11**, 141–147.
8 Y.-C. Chen and X. Fan, *Adv. Opt. Mater.*, 2019, **7**, 1900377.
9 M. Humar and S. Hyun Yun, *Nat. Photonics*, 2015, **9**, 572–576.
10 Y. Wang, K. S. Leck, V. D. Ta, R. Chen, V. Nalla, Y. Gao, T. He, H. V. Demir and H. Sun, *Adv. Mater.*, 2015, **27**, 169–175.
11 M. J. H. Tan, Y. Wang and Y. Chan, *Appl. Phys. Lett.*, 2019, **114**, 183101.
12 J. Schäfer, J. P. Mondia, R. Sharma, Z. H. Lu, A. S. Susha, A. L. Rogach and L. J. Wang, *Nano Lett.*, 2008, **8**, 1709–1712.
13 M. Kazes, D. Y. Lewis, Y. Ebenstein, T. Mokari and U. Banin, *Adv. Mater.*, 2002, **14**, 317–321.
14 M. Li, M. Zhi, H. Zhu, W.-Y. Wu, Q.-H. Xu, M. H. Jhon and Y. Chan, *Nat. Commun.*, 2015, **6**, 8513.
15 S. Delikanli, O. Erdem, F. Isik, H. Dehghanpour Baruj, F. Shabani, H. B. Yagci, E. G. Durmusoglu and H. V. Demir, *J. Phys. Chem. Lett.*, 2021, **12**, 2177–2182.

16 A. Yeltik, S. Delikanli, M. Olutas, Y. Kelestemur, B. Guzelturk and H. V. Demir, *J. Phys. Chem. C*, 2015, **119**, 26768–26775.
17 N. Taghipour, S. Delikanli, S. Shendre, M. Sak, M. Li, F. Isik, I. Tanriover, B. Guzelturk, T. C. Sum and H. V. Demir, *Nat. Commun.*, 2020, **11**, 3305.
18 S. Delikanli, G. Yu, A. Yeltik, S. Bose, T. Erdem, J. Yu, O. Erdem, M. Sharma, V. K. Sharma, U. Quliyeva, S. Shendre, C. Dang, D. H. Zhang, T. C. Sum, W. Fan and H. V. Demir, *Adv. Funct. Mater.*, 2019, **29**, 1901028.
19 S. Delikanli, B. Guzelturk, P. L. Hernández-Martínez, T. Erdem, Y. Kelestemur, M. Olutas, M. Z. Akgul and H. V. Demir, *Adv. Funct. Mater.*, 2015, **25**, 4282–4289.
20 M. İzmir, A. Sharma, S. Shendre, E. G. Durmusoglu, V. K. Sharma, F. Shabani, H. D. Baruj, S. Delikanli, M. Sharma and H. V. Demir, *ACS Appl. Nano Mater.*, 2022, **5**, 1367–1376.
21 L. T. Kunneman, M. D. Tessier, H. Heuclin, B. Dubertret, Y. V. Aulin, F. C. Grozema, J. M. Schins and L. D. A. Siebbeles, *J. Phys. Chem. Lett.*, 2013, **4**, 3574–3578.
22 S. Delikanli, F. Isik, F. Shabani, H. D. Baruj, N. Taghipour and H. V. Demir, *Adv. Opt. Mater.*, 2021, **9**, 2002220.
23 J. Yu, M. Sharma, M. Li, S. Delikanli, A. Sharma, M. Taimoor, Y. Altintas, J. R. McBride, T. Kusserow, T.-C. Sum, H. V. Demir and C. Dang, *Laser Photonics Rev.*, 2021, **15**, 2100034.
24 S. Shendre, S. Delikanli, M. Li, D. Dede, Z. Pan, S. T. Ha, Y. H. Fu, P. L. Hernández-Martínez, J. Yu, O. Erdem, A. I. Kuznetsov, C. Dang, T. C. Sum and H. V. Demir, *Nanoscale*, 2019, **11**, 301–310.
25 M. Sak, N. Taghipour, S. Delikanli, S. Shendre, I. Tanriover, S. Foroutan, Y. Gao, J. Yu, Z. Yanyan, S. Yoo, C. Dang and H. V. Demir, *Adv. Funct. Mater.*, 2020, **30**, 1907417.
26 S. Ithurria and D. V. Talapin, *J. Am. Chem. Soc.*, 2012, **134**, 18585–18590.
27 H. Htoon, J. A. Hollingworth, A. V. Malko, R. Dickerson and V. I. Klimov, *Appl. Phys. Lett.*, 2003, **82**, 4776–4778.
28 H. Htoon, J. A. Hollingsworth, R. Dickerson and V. I. Klimov, *Phys. Rev. Lett.*, 2003, **91**, 227401.
29 R. Tomar, A. Kulkarni, K. Chen, S. Singh, D. van Thourhout, J. M. Hodgkiss, L. D. A. Siebbeles, Z. Hens and P. Geiregat, *J. Phys. Chem. C*, 2019, **123**, 9640–9650.
30 D. Dede, N. Taghipour, U. Quliyeva, M. Sak, Y. Kelestemur, K. Gungor and H. V. Demir, *Chem. Mater.*, 2019, **31**, 1818–1826.
31 B. Guzelturk, Y. Kelestemur, M. Olutas, Q. Li, T. Lian and H. V. Demir, *J. Phys. Chem. Lett.*, 2017, **8**, 5317–5324.
32 C. She, I. Fedin, D. S. Dolzhnikov, P. D. Dahlberg, G. S. Engel, R. D. Schaller and D. V. Talapin, *ACS Nano*, 2015, **9**, 9475–9485.
33 O. V. Kozlov, Y.-S. Park, J. Roh, I. Fedin, T. Nakotte and V. I. Klimov, *Science*, 2019, **365**, 672–675.
34 J. Cassidy, B. T. Diroll, N. Mondal, D. B. Berkinsky, K. Zhao, D. Harankahage, D. Porotnikov, R. Gately, D. Khon, A. Proppe, M. G. Bawendi, R. D. Schaller, A. V. Malko and M. Zamkov, *ACS Nano*, 2022, **16**, 3017–3026.
35 W. K. Bae, L. A. Padilha, Y.-S. Park, H. McDaniel, I. Robel, J. M. Pietryga and V. I. Klimov, *ACS Nano*, 2013, **7**, 3411–3419.
36 Y. Kelestemur, A. F. Cihan, B. Guzelturk and H. V. Demir, *Nanoscale*, 2014, **6**, 8509–8514.
37 Y. Kelestemur, A. F. Cihan, B. Guzelturk, O. Yerli, U. Kurum, H. G. Yaglioglu, A. Elmali and H. V. Demir, Blue- and red-shifting amplified spontaneous emission of CdSe/CdS core/shell colloidal quantum dots, in *CLEO: Science and Innovations 2013*, San Jose, California, United States, 2013.
38 O. Chen, J. Zhao, V. P. Chauhan, J. Cui, C. Wong, D. K. Harris, H. Wei, H.-S. Han, D. Fukumura, R. K. Jain and M. G. Bawendi, *Nat. Mater.*, 2013, **12**, 445–451.
39 S. F. Wuister, C. de Mello Donegá and A. Meijerink, *J. Phys. Chem. B*, 2004, **108**, 17393–17397.